Southern Hemisphere Circulation Features Associated with El Niño–Southern Oscillation Events

DAVID J. KAROLY*

Centre for Dynamical Meteorology, Monash University, Clayton, Victoria, Australia

(Manuscript received 19 December 1988, in final form 27 April 1989)

ABSTRACT

Composite seasonal mean and anomaly fields prepared from operational numerical analyses have been used to describe the Southern Hemisphere (SH) circulation features associated with El Niño–Southern Oscillation (ENSO) events. The period of analyses available (1972–83) has limited the composites to include only three ENSO events. The reliability and stability of the composites has been tested using multiple permutation methods and by comparison with the results obtained using a longer period (1950–79) of SH rawinsonde station data.

In the SH winter, a weak equivalent-barotropic wavetrain pattern of anomalies extends over Australia and the South Pacific Ocean to South America. This wavetrain pattern is quite variable in amplitude and location between ENSO events, although it is more stable over the subtropical Pacific. In the SH summer, the circulation anomalies are more zonally symmetric, with increased height at low and high latitudes and decreased height in middle latitudes. The circulation anomalies in the SH summer are more stable than in winter, with similar patterns of anomalies in the subtropics and middle latitudes in all events.

1. Introduction

The largest interannual variations of the atmospheric circulation in the tropics are associated with El Niño–Southern Oscillation (ENSO) events. A number of recent studies have described the circulation features in the tropics during ENSO events and the associated anomalies in the Northern Hemisphere (NH) circulation (Horel and Wallace 1981; Rasmusson and Carpenter 1982; Arkin 1982; van Loon and Rogers 1981; and others).

The main circulation anomalies in the tropics and NH vary with the seasonal cycle. During the mature stage of an ENSO event in the NH winter, the tropical anomalies are linked to the eastward movement of the major region of convective activity from the Indonesian–west Pacific Ocean area to the central Pacific Ocean near the date line, with anomalous divergence at upper levels over the date line and anomalous convergence around 130°E. The associated anomalies in the NH circulation are an anticyclonic anomaly in the subtropics over the central Pacific and a wavetrain pattern of anomalies extending north and east over the North Pacific and North America. This wavetrain in the NH winter associated with ENSO events is often referred to as the Pacific–North American (PNA) pattern. The circulation anomalies associated with the PNA pattern are equivalent-barotropic, with increasing amplitude and small phase tilt with height in the upper troposphere. At earlier stages in the development of an ENSO event, the NH circulation anomalies are weaker and less extensive, with the major stable feature being an anomalous anticyclone over the subtropical Pacific Ocean.

Fewer studies have considered the circulation features in the Southern Hemisphere (SH) associated with ENSO events, e.g., Trenberth (1976), van Loon and Rogers (1981), van Loon (1984), van Loon and Shea (1987); these have generally concentrated on features at low levels or in the NH winter (SH summer) season. They have described the seasonal evolution of the surface pressure anomalies, including the positive anomalies over Australia and the Indian Ocean and negative anomalies over the eastern Pacific Ocean. Arkin (1982) has shown that anticyclonic circulation anomalies exist at upper levels in the subtropical SH over the central Pacific Ocean, forming an anticyclone pair straddling the anomalous convective activity near the date line over the equator.

In this study, the circulation features in the SH troposphere associated with ENSO events are described using composite fields prepared from operational numerical analyses. Emphasis has been placed on the anomalies in the middle and upper troposphere in the

* On leave at the Atmospheric and Oceanic Sciences Program, Princeton University, Princeton, New Jersey till July, 1989.

Corresponding author address: David J. Karoly, Centre for Dynamical Meteorology, Monash University, Clayton, Victoria 3168 Australia.

summer and winter seasons and comparison with the NH anomalies. The short period of analyses available (1972–83) has limited the composites to include only three ENSO events. In the SH winter (NH summer), a weak and variable wavetrain pattern of anomalies extends from Australia and the South Pacific Ocean to South America, which is analogous to the PNA pattern. During the following SH summer (NH winter), there are larger amplitude circulation anomalies in the SH, which are primarily zonally symmetric and not wavelike.

In the next section, the data used for the composites and the analysis techniques are described. Then, the SH circulation features associated with ENSO events identified in the composites are presented and contrasted with those in the NH. The stability and reliability of the composite anomalies is discussed and the composite anomalies are compared with those in each ENSO event.

2. Data

Daily numerical analyses for the SH from the World Meteorological Centre, Melbourne for the period June 1972 to December 1983 have been used. Geopotential height, temperature and wind components on seven pressure levels and mean sea level pressure were available on a polar-stereographic grid over the SH with a horizontal resolution of about 500 km. A time series of the monthly mean fields was prepared from the daily analyses. The 10-year means of the monthly mean fields for each calendar month for the period September 1972 to August 1982 were used as the climatological means. This climatology and the methods used to prepare the daily analyses have been described by Le Marshall et al. (1985) and Karoly et al. (1986). Time series of monthly mean anomalies were prepared by subtracting the 10-year mean monthly means from the individual monthly means.

During the period for which the daily SH analyses were available, three ENSO events occurred; in 1972, 1976/77 and 1982. The event starting in 1976 extended for two years. Seasonal mean fields and anomalies have been prepared for each of the four SH winters [June, July, August (JJA)] during these ENSO event years; 1972, 1976/77 and 1982, and the following summers [December, January, February (DJF)]. Composite seasonal means and anomalies were obtained as a simple average of the fields for the four seasons in the three ENSO events.

The reliability of the daily SH analyses has been assessed by Swanson and Trenberth (1981), Le Marshall et al. (1985) and Karoly and Oort (1987). The results from these studies have shown that the monthly mean fields are more reliable than the daily analyses, but that there are deficiencies in some of the fields. In particular, the temperature fields at low levels (850 hPa and below) and all fields at low latitudes (equatorward of about 15°S) have known analysis problems. In the results which follow, attention will be focused on mean sea level pressure, geopotential height at 500 and 200 hPa and wind at 200 hPa.

The primary constraint on the reliability of these fields is the poor data coverage over much of the Southern Hemisphere, with few conventional upper air stations and, prior to 1976, no satellite temperature soundings included in the analyses. There is no reliable way to test the results obtained here in regions without conventional upper air stations such as over most of the South Pacific Ocean.

3. Composite fields

a. Southern Hemisphere winter

During the developing stage of an ENSO event which typically occurs in the SH winter (JJA), there are small but increasing anomalies of sea surface temperature and convective activity in the central equatorial Pacific Ocean (Rasmusson and Carpenter 1982). The composite SH winter mean sea level pressure (MSLP) and 200 hPa wind speed for the three ENSO events (1972, 1976/77 and 1982) are shown in Fig. 1 and the composite anomalies of MSLP, height at 500 and 200 hPa and wind at 200 hPa are shown in Fig. 2. At the surface, the typical ENSO pattern at low latitudes of positive pressure anomalies over Australia and negative anomalies over the Pacific Ocean is clearly shown and extends into middle latitudes. This pattern has been described by van Loon and Shea (1987) and Fig. 2a is very similar to their Fig. 1f (for MJJ rather than JJA), which was prepared using data for a larger number of ENSO events.

In middle latitudes, the anomalies are equivalent barotropic, with a similar pattern at all levels. At low latitudes, there are changes to the height anomalies in the upper troposphere, above 500 hPa, so that there is an anticyclonic anomaly in the subtropics over the date line. This is associated with the extension of the subtropical westerly jet over Australia further east over the Pacific Ocean and westerly anomalies of more than 7 m s^{-1} are found at the eastern end of the jet. In the upper troposphere, there is a wavetrain pattern of height anomalies extending from this anticyclone in the subtropics over the date line poleward over the South Pacific to South America, with negative anomalies centered at 35°S, 150°W, positive anomalies at 60°S, 120°W and negative anomalies at 45°S, 60°W. Mo and Ghil (1987) have identified a similar wavetrain in the SH using daily SH winter analyses and called it the Pacific–South American (PSA) pattern. This wavetrain pattern of anomalies in the SH winter is analogous to, but much weaker than, the PNA pattern in the following NH winter. Although it is difficult to compare the magnitudes of composite anomalies, the SH height anomalies in Fig. 2 are typically half as large as those in the composites of Wallace and Gutzler (1981).

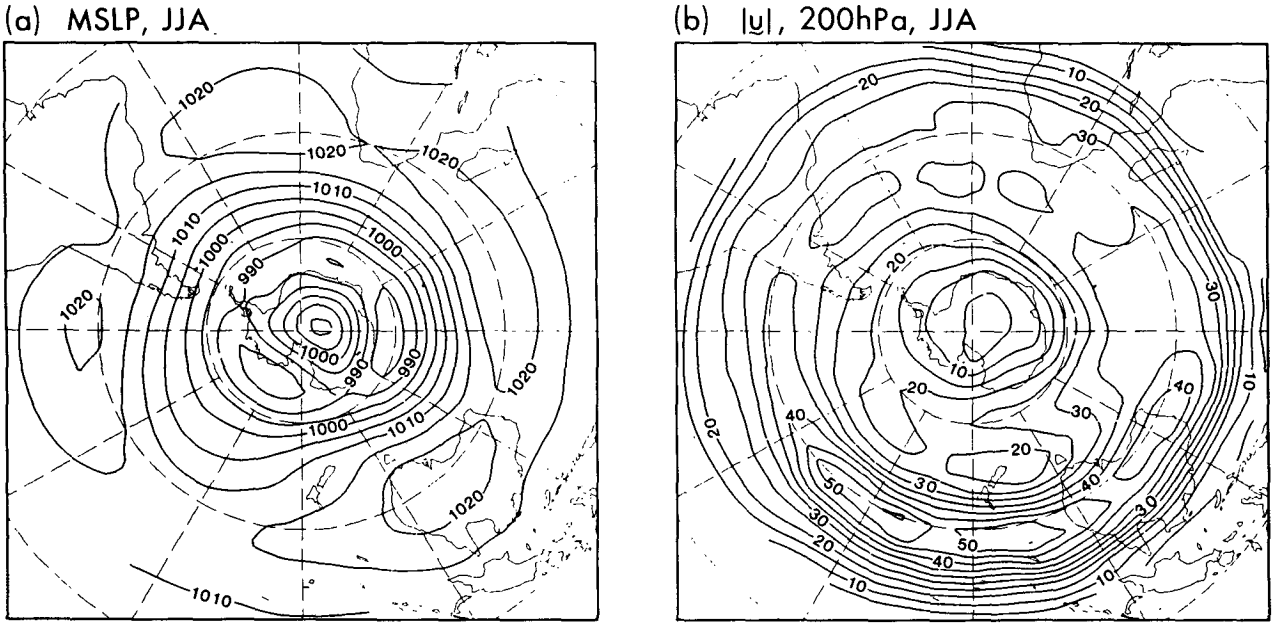

FIG. 1. Composite winter (JJA) mean fields for three ENSO events (1972, 1976/77 and 1982) of (a) mean sea level pressure (hPa) and (b) 200 hPa wind speed (m s^{-1}). Lines of latitude and longitude are drawn at 30° intervals with the Greenwich meridian at the top. Contours have been truncated at the 10°S latitude circle.

The smaller values of the wind anomalies at low latitudes equatorward of 15°S, in Fig. 2d, are likely to be an artifact of the climatological constraint used in the numerical analysis scheme which limits the departures of the wind from its climatological value at low latitudes. Thus the magnitudes of wind anomalies at low latitudes are likely to be underestimated, but the pattern of the wind anomalies should be realistic.

b. Southern Hemisphere summer

In the following SH summer (DJF), the ENSO events have typically reached their mature stage, with large positive sea surface temperature anomalies in the central equatorial Pacific Ocean (Rasmusson and Carpenter 1982). The composite MSLP and 200 hPa wind fields for the three ENSO events are shown in Fig. 3 and the composite MSLP, height and upper tropospheric wind anomalies are shown in Fig. 4.

Again, the typical ENSO pattern for MSLP at low latitudes is shown clearly but the positive anomalies of MSLP over Australia are confined to lower latitudes than in the preceding winter. There are extensive regions of negative MSLP anomalies throughout the Pacific, Indian and Atlantic oceans in middle latitudes and positive pressure anomalies at high latitudes. The composite summer MSLP anomalies in Fig. 4a are very similar to those presented by van Loon and Shea (1987) in their Fig. 1h (for NDJ rather than DJF).

This pattern of mainly zonally symmetric anomalies is more apparent at higher levels, with positive height anomalies throughout the subtropics and the largest anomalies over the subtropical Pacific Ocean, negative height anomalies in middle latitudes except over South America and smaller positive anomalies again at high latitudes. There is an anomalous subtropical jet over the Pacific Ocean, associated with westerly anomalies up to 10 m s^{-1}, which only occurs in the SH summer during ENSO events. There are westerly anomalies around the whole hemisphere at 30°S and weaker easterly anomalies at 55°S. These anomalies in the SH summer are larger than in the previous winter and are comparable in magnitude with the simultaneous anomalies in the NH winter circulation.

The magnitude of these zonally symmetric anomalies can be seen more clearly in Fig. 5, which shows the zonal mean composite anomalies of height, temperature and zonal and meridional wind in the summer. As noted earlier, there are zonal mean positive height anomalies in the subtropics and at high latitudes and negative anomalies in middle latitudes. These are associated with positive temperature anomalies at low latitudes and negative anomalies in middle latitudes. The zonal mean positive temperature anomalies and increased heights in the tropical upper troposphere during the mature stage of ENSO events have been noted by Horel and Wallace (1981). In geostrophic balance with the height anomalies are zonal mean westerly wind anomalies of 3 m s^{-1} at 25°S and easterly anomalies of 2 m s^{-1} at 55°S. In addition, an enhanced direct Hadley circulation is shown by the zonal mean meridional wind anomalies. It is likely that the wind

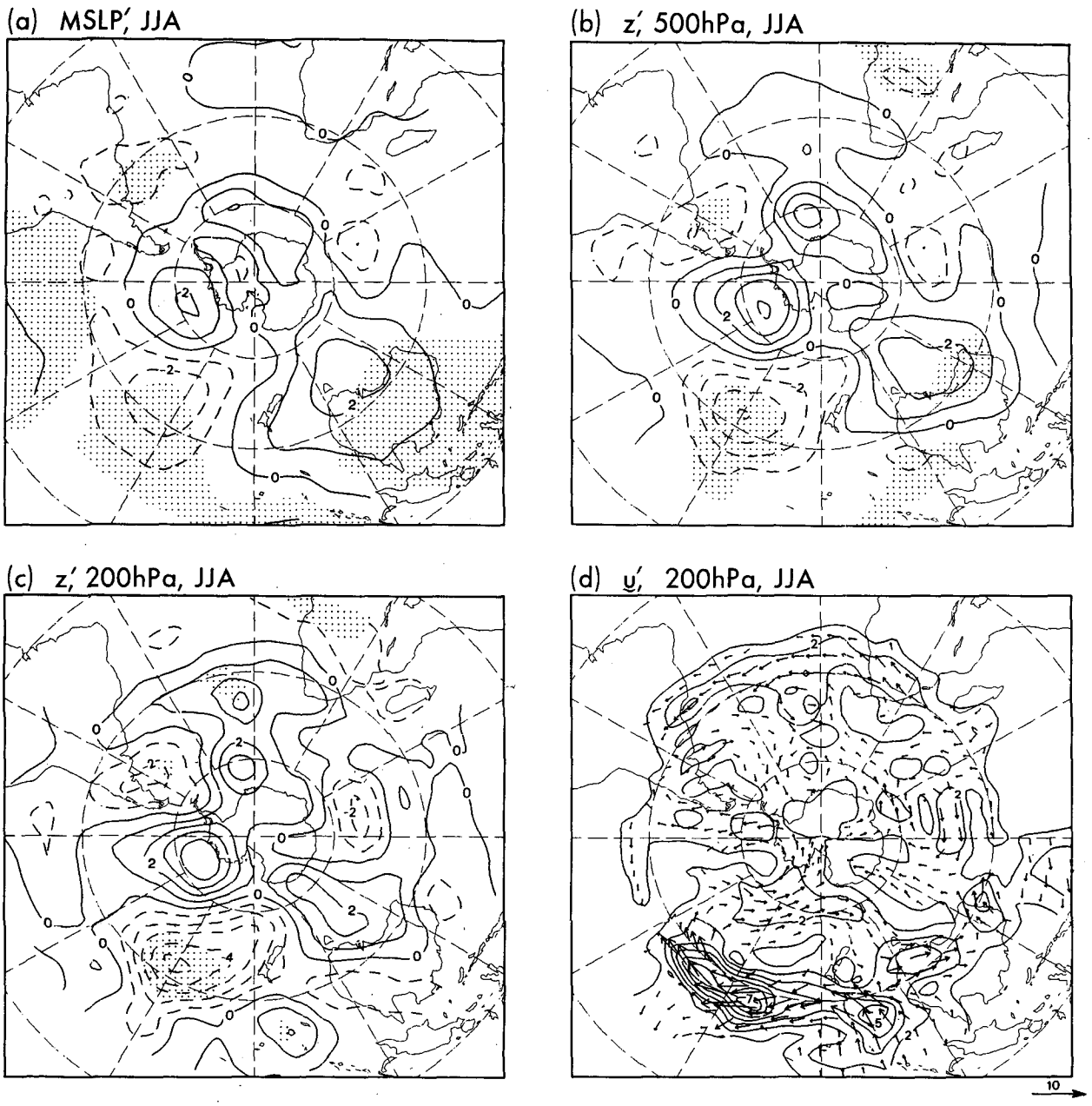

FIG. 2. Composite winter anomalies for three ENSO events for (a) mean sea level pressure (hPa), (b) 500 hPa height (dam), (c) 200 hPa height (dam) and (d) 200 hPa wind (m s^{-1}). Negative contours are drawn dashed. In (a), (b) and (c), anomalies which are significant at the 95% level using a pointwise multiple permutation test have been shaded (see section 4 for a description of this test).

anomalies at low latitudes are underestimated by the analyses used here due to the constraints in the analysis scheme described earlier.

Mo and White (1985) have described the SH summer zonally symmetric anomaly pattern at 500 hPa associated with the Southern Oscillation using the first eight years (1972–80) of the Australian analyses (see their Fig. 14). They identified the increased heights at low latitudes and reduced heights in middle latitudes during an ENSO event.

4. Reliability of the composite fields

The composite fields described in the previous section have been prepared from a very short period of data. An assessment of the reliability and stability of these composites has been carried out in several ways.

First, an attempt has been made to determine whether the composite anomaly fields are extreme or whether other randomly selected composites would give similar magnitude anomalies in the same regions.

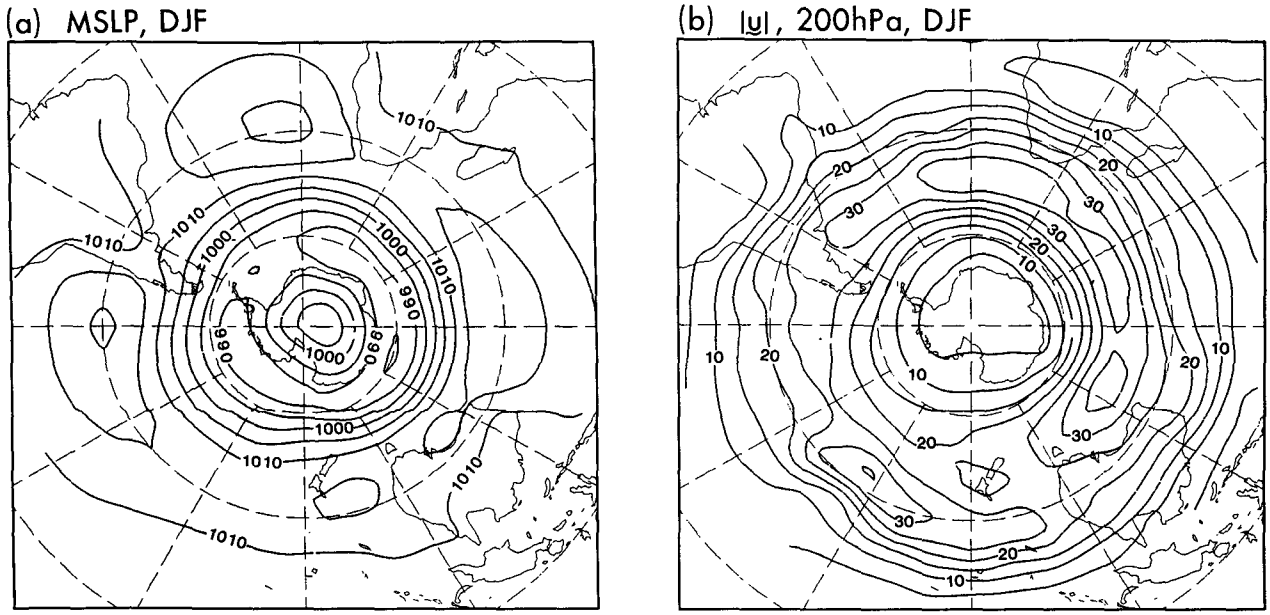

FIG. 3. Composite ENSO mean fields for the following summer (DJF) season, as in Fig. 1.

This has involved a multiple permutation technique applied to the individual seasonal mean anomalies.

The composite ENSO seasonal anomalies were obtained as the average of the four seasonal anomalies in the three ENSO events which occurred in the period June 1972–December 1983. The distributions of all possible four-season composite anomalies for winter and summer were generated from the available data at individual gridpoints. There were 495 possible four-winter composites from the 12 winters available and 330 possible four-summer composites from the 11 summers available. The frequency distributions of possible four-season composite anomalies for 500 hPa height in winter and summer at selected gridpoints are shown in Figs. 6 and 7. The gridpoints were chosen because they had large anomalies for the ENSO composites. The magnitudes of the four-season composite anomalies have been normalized by their standard deviations, giving normalized distributions. In all cases, the distributions of composite anomalies are not significantly different from the normal distribution.

At the selected gridpoints for the winter composites, the ENSO composite anomaly lies in the extreme tail of the distribution. At two of the points (Figs. 6b and 6c), the ENSO composite is the largest magnitude anomaly of all the four-season composites at that point. For the summer composites, at all four selected points, the ENSO composite is the largest magnitude anomaly. This indicates that the ENSO composite anomalies are extreme in magnitude and do not arise from a single ENSO event.

This multiple permutation method has also been used to provide a measure of how extreme the ENSO composites are over the whole hemisphere. The standard deviation of the multiple permutation distribution of all possible four-season composites was computed at every gridpoint. Since these multiple permutation distributions are approximately normal (see above), comparison of the composite ENSO anomaly with the standard deviation gives a measure of the significance of the anomaly, i.e., composite ENSO anomalies with magnitudes greater than two standard deviations will be larger than about 95% of the possible four-season composite anomalies. Regions with anomalies larger than two standard deviations have been shaded in Figs. 2 and 4.

The composite winter anomalies in Fig. 2 have magnitudes larger than two standard deviations over the Pacific Ocean in subtropical and middle latitudes. In the upper troposphere, most of the centers of the wavetrain pattern have "extreme" anomalies. At high latitudes, however, the composite anomalies do not exceed two standard deviations, indicating that they are not large compared with other possible four-season composite anomalies. The composite summer anomalies in Fig. 4 have much larger areas with magnitudes greater than two standard deviations, including most of the SH in subtropical and middle latitudes.

Another test of the reliability of the composite seasonal anomaly patterns is their comparison with the individual seasonal anomalies during each of the ENSO events, which are shown in Figs. 8 and 9 for the 500 hPa height anomalies. There are large variations of the seasonal anomalies in winter between the events, with a few features apparent in all (or most) cases. These include positive anomalies over Australia, negative anomalies in middle latitudes around 150°W and positive anomalies at higher latitudes around 90°W. In

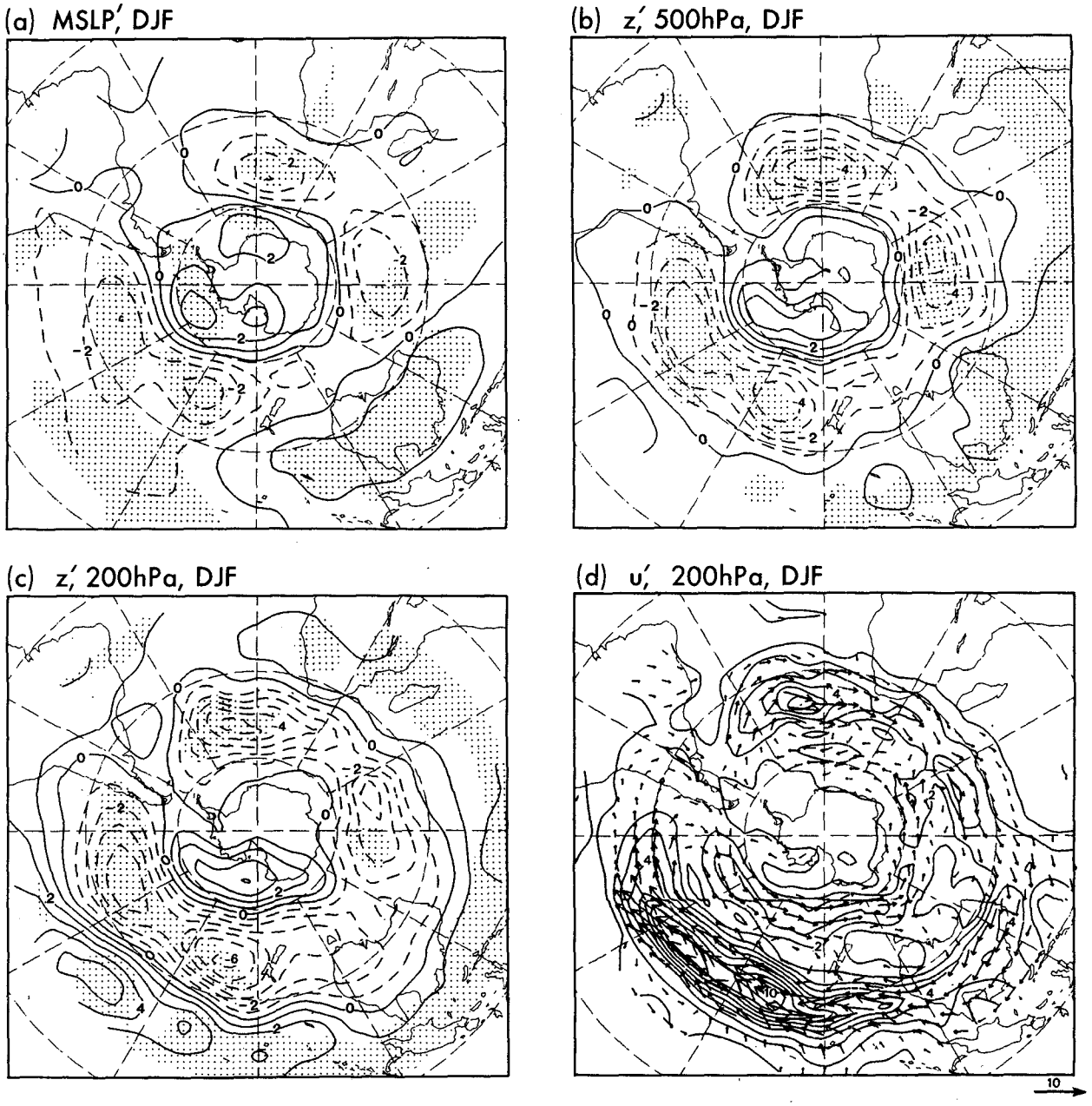

FIG. 4. Composite ENSO anomalies for the following summer (DJF) season, as in Fig. 2.

winter, the anomalies have a wavelike pattern. The seasonal anomalies in summer are more stable and zonally symmetric, with positive anomalies in the subtropics and negative anomalies in middle latitudes in all cases, although the anomalies at high latitudes are variable.

These two tests indicate that the SH circulation features in the winter of a developing ENSO event are stable in low latitudes in the Pacific region but quite variable at middle and high latitudes. During the SH summer, in the mature stage of an ENSO event, the circulation features are stable in low and middle latitudes around the whole hemisphere but are more variable at high latitudes.

The period of data which has been used to prepare the composite anomalies is very short, only 12 years. It is possible to use SH radiosonde station data, available since 1950, to verify the composite ENSO circulation features over a longer period in some regions. Szeredi and Karoly (1987) have described the horizontal structure of monthly variations of the SH circulation using radiosonde station data for the period

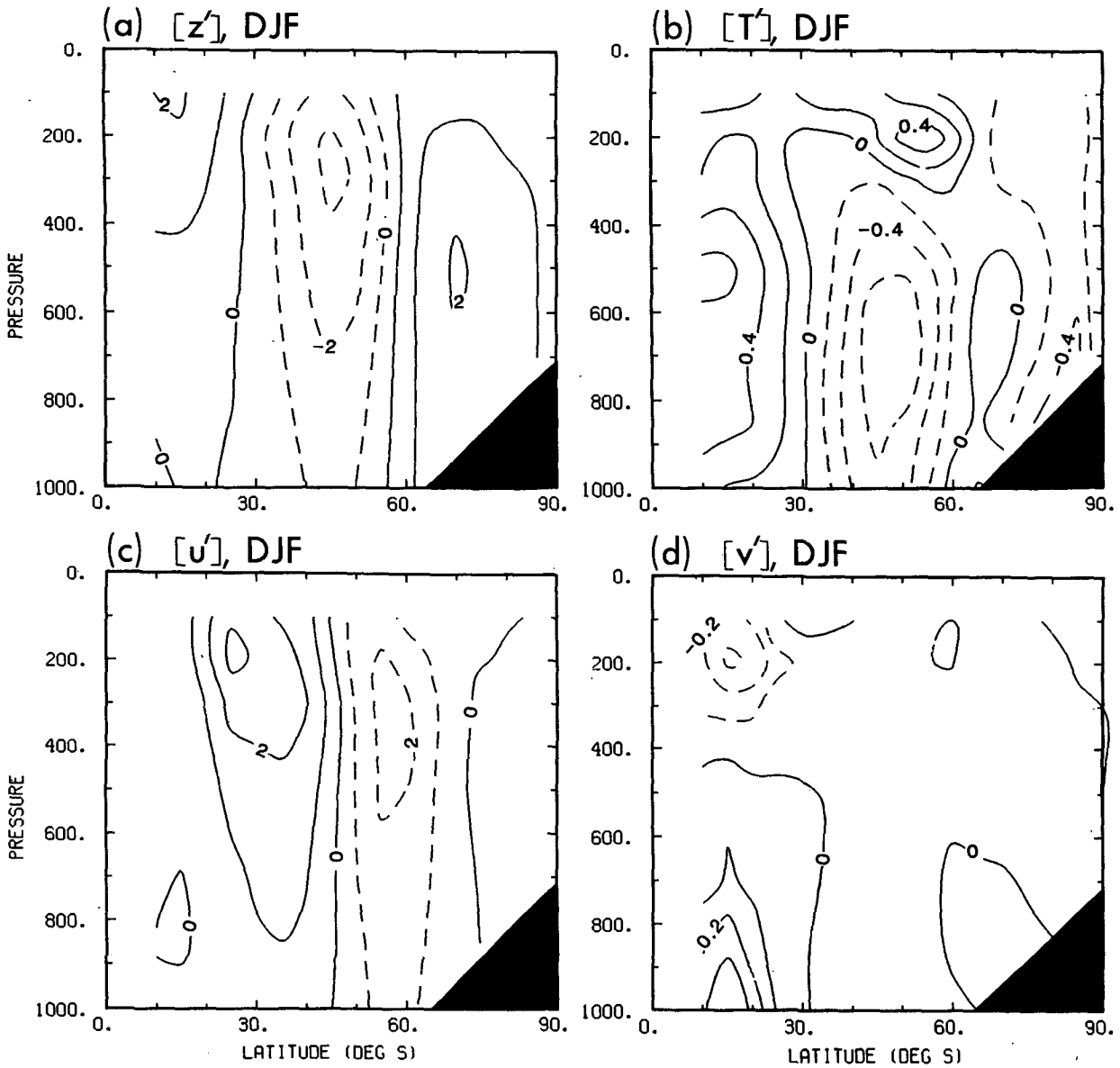

FIG. 5. Zonal mean composite ENSO summer anomaly fields for (a) height (dam), (b) temperature (°C), (c) zonal wind (m s^{-1}) and (d) meridional wind (m s^{-1}).

1950–1979. They found an anomaly pattern in the summer that is very similar to the composite ENSO anomaly described here and that had large negative correlations with the Southern Oscillation Index (Tahiti minus Darwin normalized monthly pressure anomalies). This anomaly pattern was primarily zonally symmetric, with increased heights in the upper troposphere everywhere at low latitudes (with largest amplitudes over the Pacific Ocean), westerly wind anomalies in the subtropics over the Pacific Ocean and negative height anomalies in middle latitudes. Thus the ENSO composite anomalies in summer can be verified over a longer period with this station data. In winter, however, Szeredi and Karoly (1987) did not find a coherent hemispheric pattern of anomalies in the radiosonde station data associated with ENSO events. This may have been due to the sparse and irregular network of SH radiosonde stations, particularly over the eastern Pacific Ocean and South America. Thus, it is not possible to verify the ENSO composite anomalies in winter using radiosonde station data.

5. Discussion

During an ENSO event in the SH summer, there are stable zonally symmetric anomalies of the SH cir-

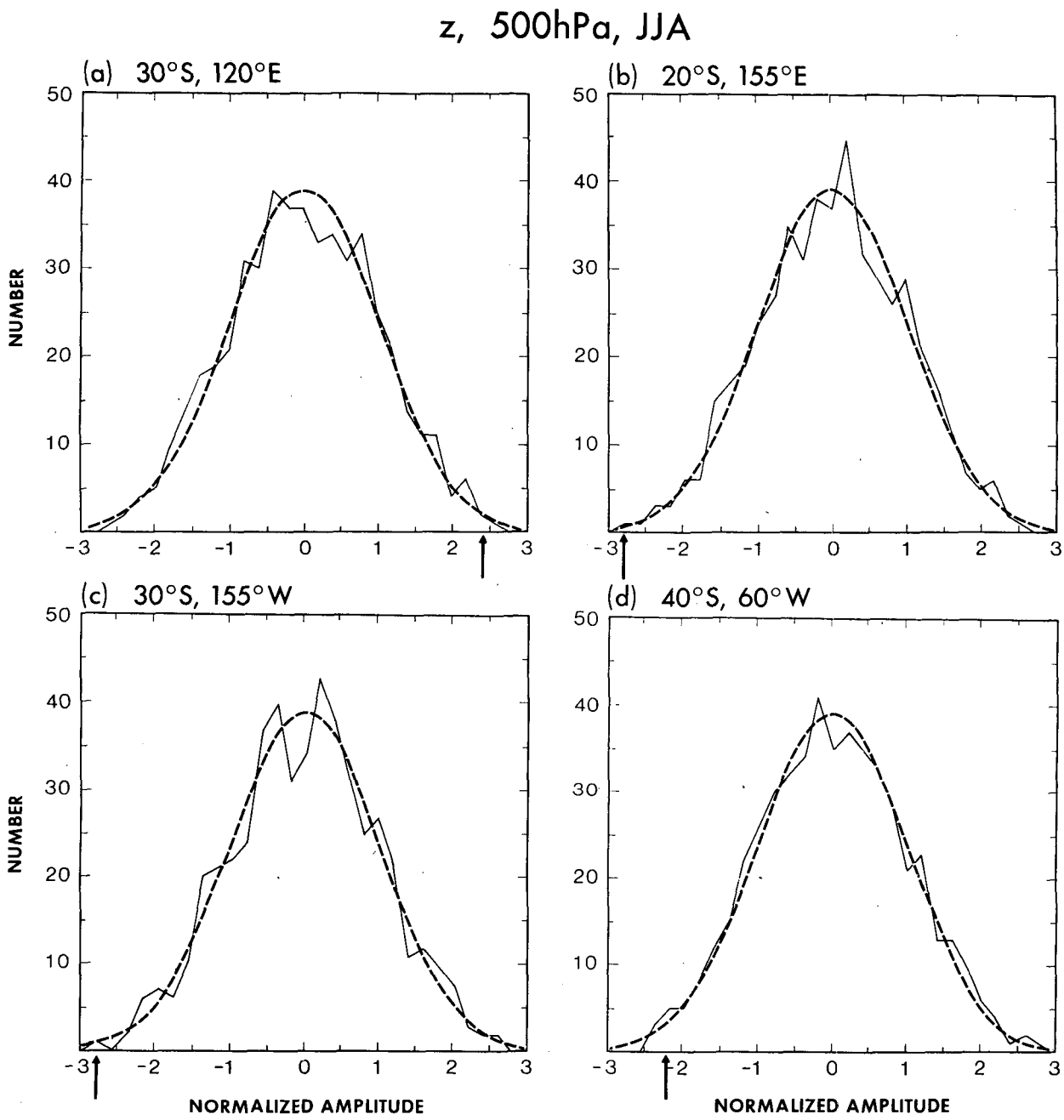

FIG. 6. Frequency distribution of all possible four-season composite winter anomalies of 500 hPa height generated using the multiple permutation method at four selected gridpoints. The abscissa is the amplitude of the composite anomaly normalized by dividing by the standard deviation of all the 495 possible composite anomalies. The normal distribution for the same number of cases is shown by the dashed line. For each distribution, the magnitude of the composite ENSO anomaly has been indicated by an arrow.

culation with increased height and temperature at low latitudes and decreased height in middle latitudes. During the preceding SH winter, the circulation anomalies are more variable but appear to be associated with a wavetrain pattern of anomalies extending poleward and eastward over the Pacific Ocean. The greater variability of the anomalies in the SH winter may be associated with the weaker and more geographically variable sea surface temperature anomalies in the central equatorial Pacific Ocean in the developing stage of an ENSO event than in the mature stage.

The wavetrain circulation anomalies in the SH win-

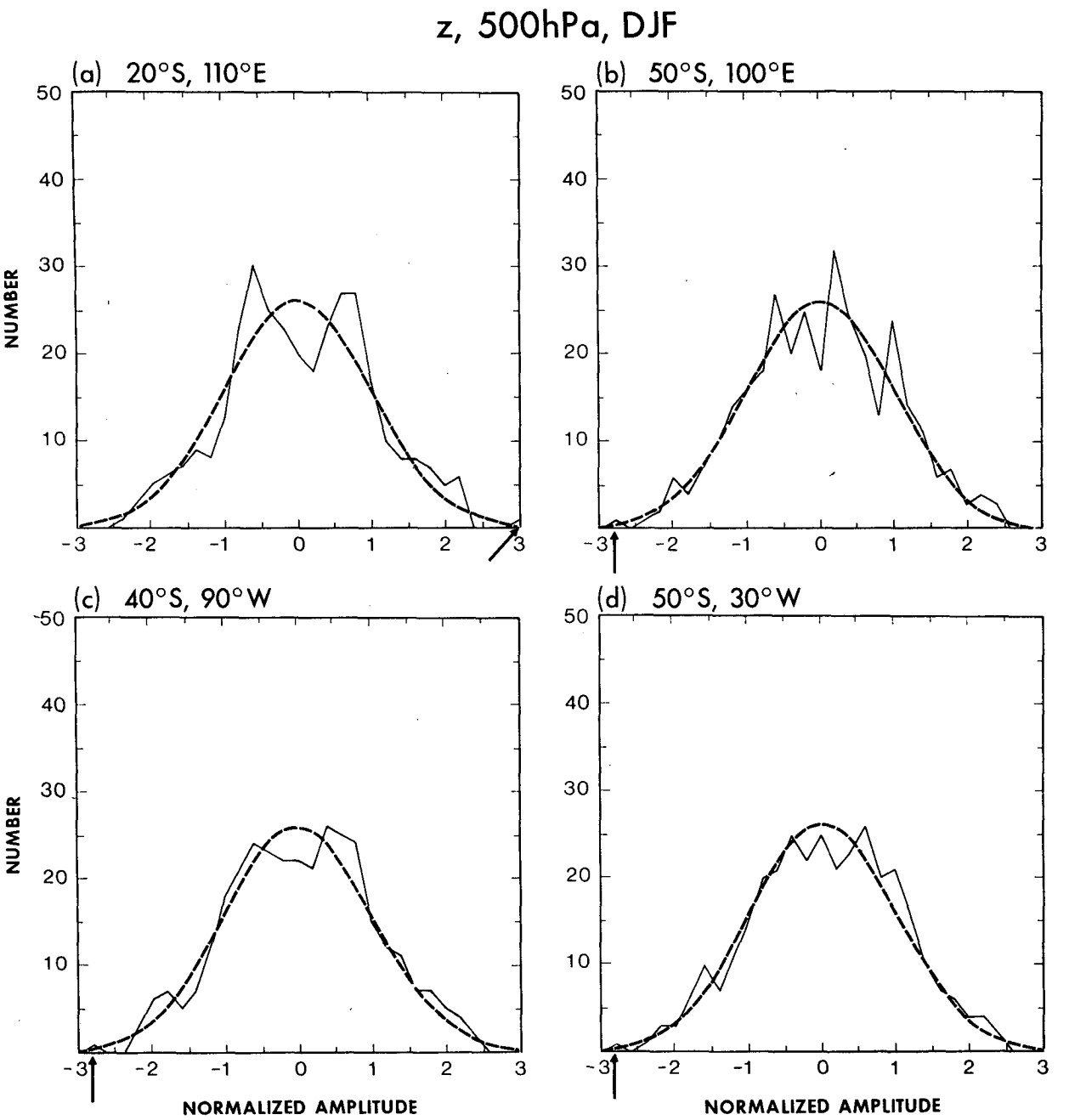

FIG. 7. As in Fig. 6, but for composite summer anomalies, with a total of 330 possible composites in the distribution.

ter are consistent with the Rossby wave response to anomalous low latitude forcing (Hoskins and Karoly 1981). Theory would suggest that the wavetrain response should be larger in the winter hemisphere than in the summer hemisphere for the same tropical forcing, as found in the ENSO composites for the SH described here and in the NH described by Horel and Wallace (1981).

A number of general circulation modeling experiments have been performed to investigate the atmospheric response to equatorial sea surface temperature anomalies associated with ENSO events, e.g., Palmer and Mansfield (1986), Blackmon et al. (1983), Lau (1985). These experiments have generally used NH winter conditions and have concentrated on the results in the tropics and the NH. It is illustrative to compare

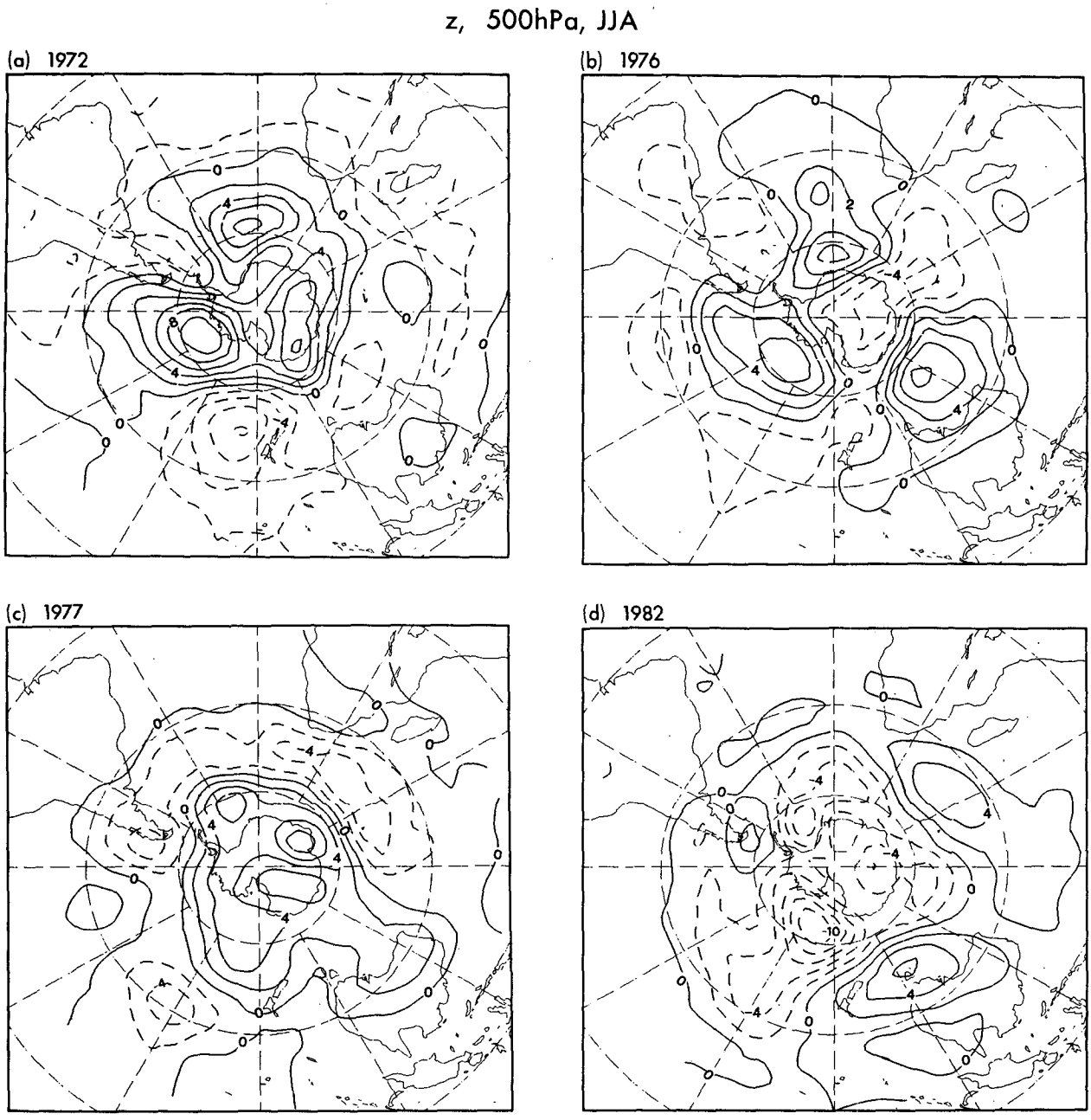

FIG. 8. Seasonal mean winter (JJA) anomalies of 500 hPa height (dam) for (a) 1972, (b) 1976, (c) 1977 and (d) 1982.

their published results for the circulation anomalies in the SH with the observed composite anomalies described here. In the NH winter (SH summer), the modeling results are usually similar to the observed composite anomalies, with primarily a zonally symmetric pattern of increased heights at low latitudes and reduced heights in middle latitudes (e.g., Palmer and Mansfield 1986, Fig. 14a).

Although there have been few of these modeling studies for SH winter (NH summer) conditions, Keshavamurty (1982) in such a study has shown a wavetrain pattern of anomalies extending poleward and eastward across the South Pacific Ocean from the anomalous tropical forcing into the winter (Southern) hemisphere (see his Fig. 8).

After completion of the analysis reported here, a complementary study of low frequency variations of the SH circulation was completed using a longer period

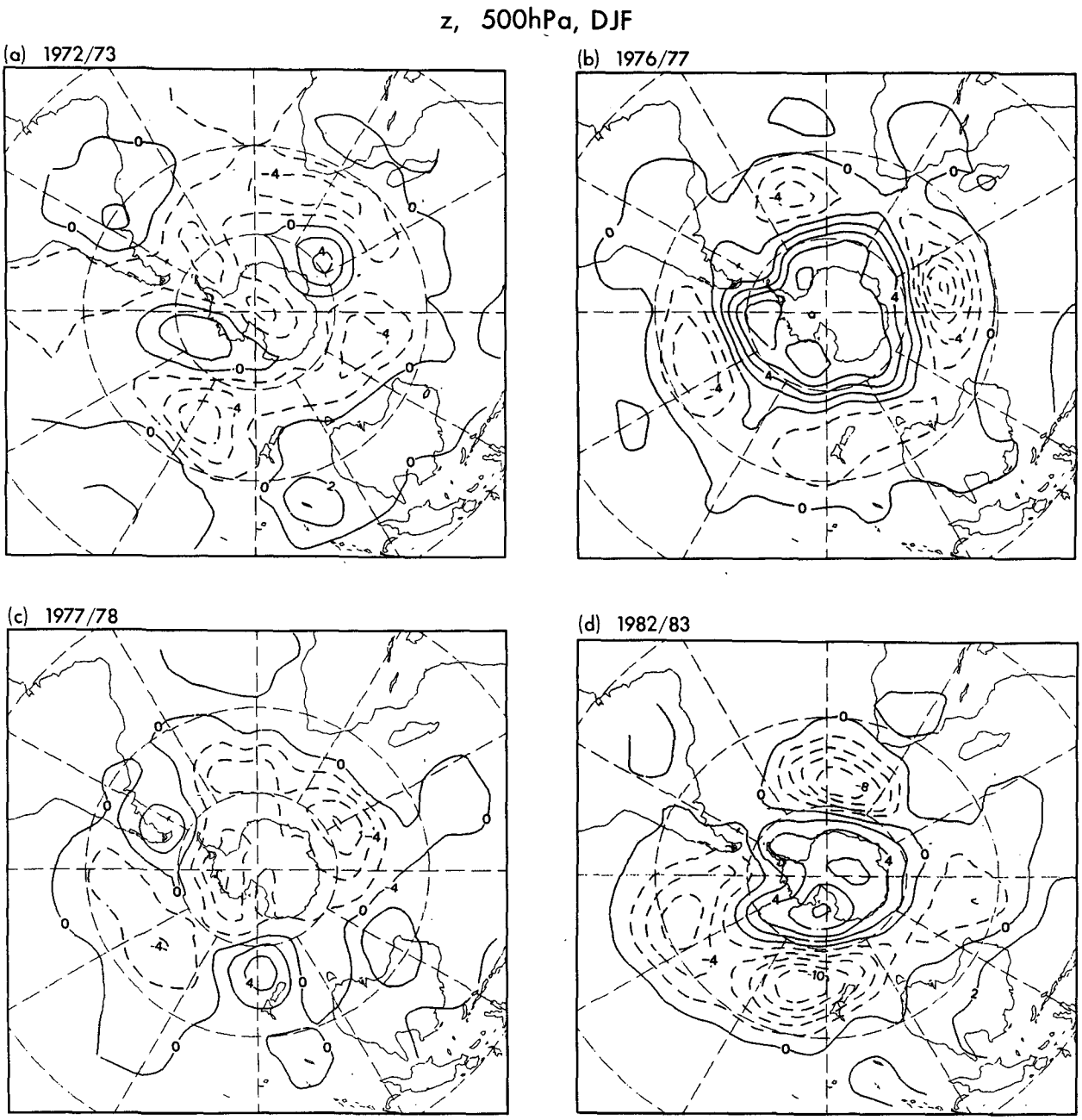

FIG. 9. Seasonal mean summer (DJF) anomalies of 500 hPa height (dam) for (a) 1972/73, (b) 1976/77, (c) 1977/78 and (d) 1982/83.

of SH numerical analyses by Szeredi (1987). He showed that the correlation between the seasonal mean Southern Oscillation Index (normalized difference between monthly mean pressures at Tahiti and Darwin) and the seasonal mean 200 hPa height for the period 1972–87 (shown in his Fig. 5.10) has a very similar pattern to the composite ENSO height anomalies. This is not surprising due to the large overlap of data used, but the correlation results include all years with both positive and negative values of the SOI, not just ENSO events.

In addition to the three ENSO events during the period 1972–83 that were used in this analysis, another ENSO event has occurred more recently. This event lasted from the second half of 1986 to the beginning of 1988. Seasonal mean 500 hPa height anomalies

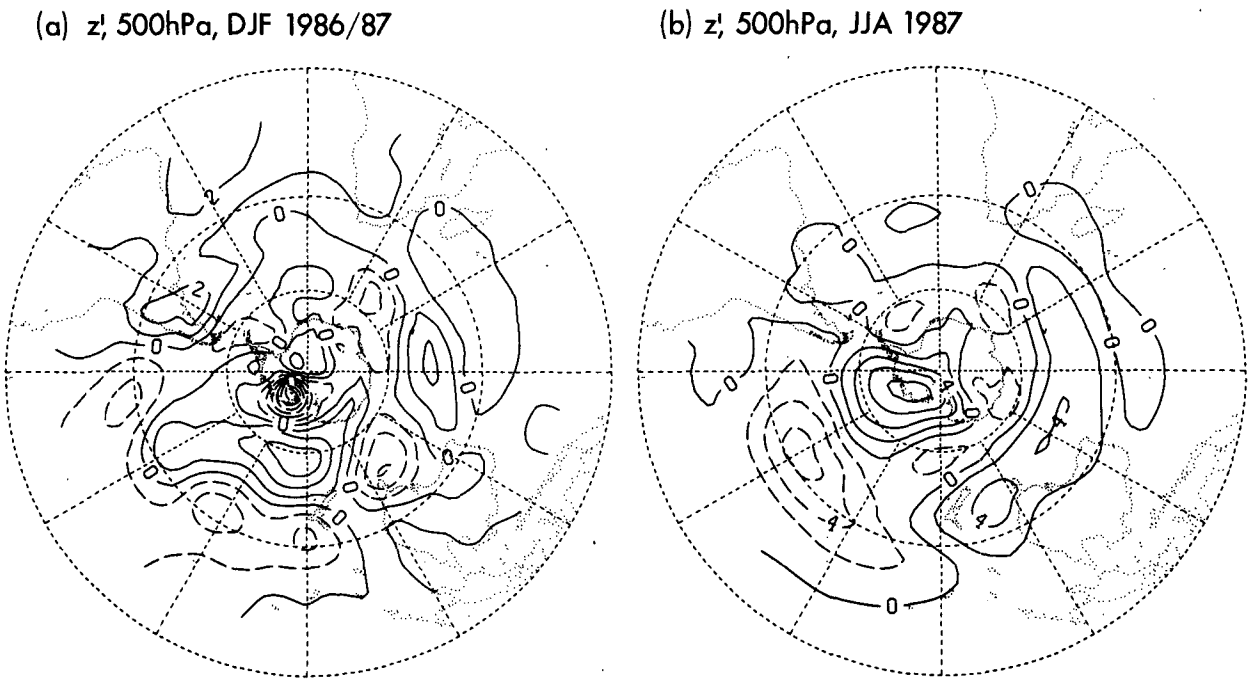

FIG. 10. Seasonal mean anomalies of 500 hPa height for (a) summer (DJF) 1986/87 (contour interval 1 dam) and (b) winter (JJA) 1987 (contour interval 2 dam) from ECMWF analyses. The base period for computing the anomalies is 1980–87.

computed using ECMWF analyses are shown in Fig. 10 for SH summer 1986/87 and winter 1987. Anomalies for the following summer, 1987/88, are not shown as the analyses were not available. The summer anomalies are weaker and less zonally symmetric than those in Fig. 9, possibly because this ENSO event developed later in the calendar year. The anomalies for the following summer, 1987/88, during the mature state of this ENSO event, show a more zonally symmetric pattern, with increased height in the subtropics and reduced heights in middle latitudes (Halpert 1988, Fig. 13), as in the composite summer anomalies. The winter anomalies (Fig. 10b) have a very similar pattern to the winter composite anomalies, with positive anomalies over southern Australia and the wavetrain pattern of anomalies of alternating sign extending from the subtropical Pacific over the date line to the South Atlantic Ocean. Thus, the SH height anomalies during the early stages of this ENSO event in summer, 1986/87, do not fit the composite pattern well, but during the following winter and summer, they are quite similar to the composite anomalies.

Horel and Wallace (1981) used their observational results to prepare a schematic illustration of the pattern of upper tropospheric anomalies in the tropics and NH associated with an ENSO event during the NH winter. Figure 11 shows an extension (and rotation) of this illustration (their Fig. 11) to include more of the SH and the SH winter season. During the SH winter (JJA), typically in the developing stage of an ENSO event, a pair of anticyclonic circulation anomalies in the upper troposphere in the subtropics straddles the anomalous equatorial convection. A weak wavetrain pattern of anomalies extends poleward and eastward across the South Pacific Ocean. At this stage, there is no coherent pattern of anomalies in the extratropical NH, except over the North Pacific Ocean. During the SH summer (DJF), typically in the mature stage of an ENSO event, the circulation anomalies are as shown in Horel and Wallace (1981), with a stronger pair of anticyclonic anomalies straddling the anomalous equatorial convection and a wavetrain of anomalies extending across the North Pacific Ocean to North America. In the SH, the circulation anomalies are larger than in the preceding winter and more zonally symmetric, with positive anomalies at low latitudes and negative anomalies in middle latitudes.

Figure 11 is based on the composite circulation anomalies described here and by Horel and Wallace (1981) for a "typical" ENSO event evolution, starting early one year and lasting for about 12 months. There are large variations between events in their timing, duration and amplitude, as shown by the weak two-year event during 1976/77 and the unusual timing of the recent 1986–88 event. This means that the composite anomalies may not represent well the seasonal anomalies in any individual event, as illustrated in Figs. 8–10.

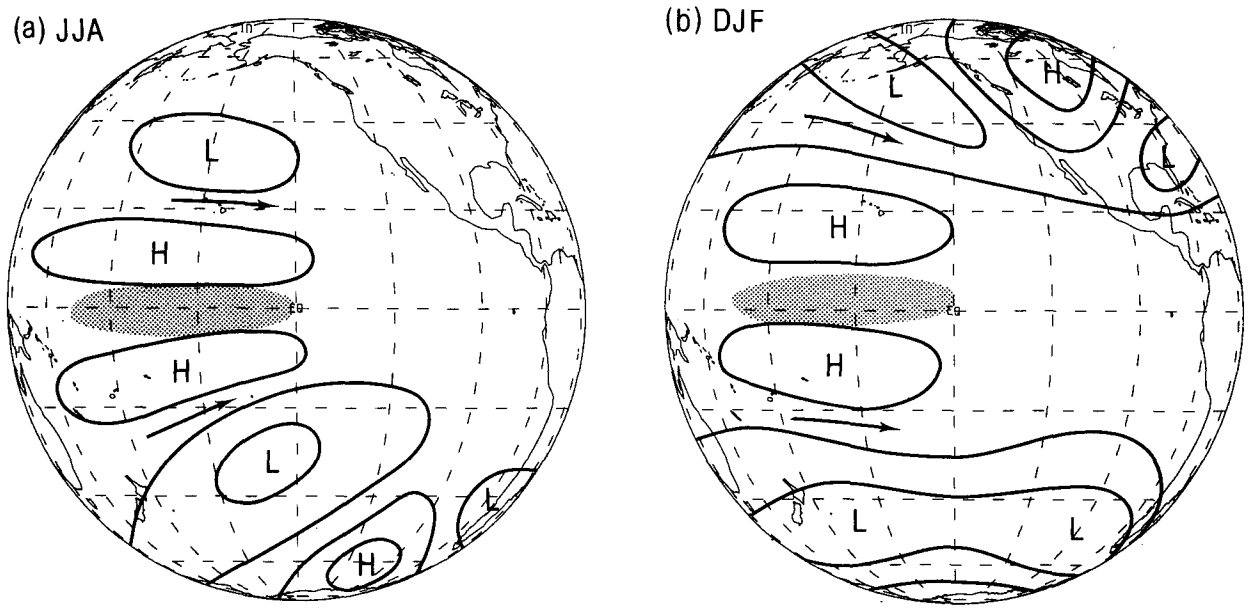

FIG. 11. Schematic illustration of the pattern of upper tropospheric height anomalies over the Pacific Ocean during (a) the early stage of an ENSO event in the SH winter (JJA) and (b) the mature stage of an ENSO event in the SH summer (DJF). The stippling shows the region of enhanced convection over the central equatorial Pacific and the arrows indicate the westerly wind anomalies in the jet streams.

It must be stressed that the results presented here are based on a very short period of data and that large variations of the SH circulation features may be associated with ENSO events during different periods. In particular, the circulation features at high latitudes are quite variable within the period of analysis. More reliable results will have to wait until a much longer period of data is available.

Acknowledgments. Part of this study was completed while the author was visiting the National Center for Atmospheric Research in 1985 and some preliminary results were presented then (Karoly 1985). Discussions with Kevin Trenberth, Harry van Loon and Kingtse Mo have been of great benefit. This research has been supported in part by a grant from the Australian Research Grants Scheme. I wish to thank Alison Leicester for typing the manuscript and Jean Sheldon for preparing the diagrams.

REFERENCES

Arkin, P. A., 1982: The relationship between interannual variability in the 200 mb tropical wind field and the Southern Oscillation. *Mon. Wea. Rev.*, **110,** 1393–1404.

Blackmon, M. L., J. E. Geisler and E. J. Pitcher, 1983: A general circulation model study of January climate anomaly patterns associated with interannual variations of equatorial Pacific sea surface temperatures. *J. Atmos. Sci.*, **40,** 1410–1425.

Halpert, M. S., 1988: The global climate for December, 1987–February, 1988. *J. Climate,* **1,** 627–652.

Hoskins, B. J., and D. J. Karoly, 1981: The steady linear response of a spherical atmosphere to thermal and orographic forcing. *J. Atmos. Sci.*, **38,** 1178–1196.

Horel, J. D., and J. M. Wallace, 1981: Planetary-scale atmospheric phenomena associated with the Southern Oscillation. *Mon. Wea. Rev.*, **109,** 813–829.

Karoly, D. J., 1985: Southern Hemisphere circulation anomalies associated with ENSO events. *Trop. Ocean–Atmos. Newslett.*, No. 33, 19.

——, and A. H. Oort, 1987: A comparison of Southern Hemisphere circulation statistics based on GFDL and Australian analyses. *Mon. Wea. Rev.*, **115,** 2033–2059.

——, G. A. M. Kelly, J. F. Le Marshall and D. J. Pike, 1986: An atmospheric climatology of the Southern Hemisphere based on ten years of daily numerical analyses (1972–82). WMO Long-Range Forecasting Research Report No. 7, WMO/TD-No. 92, 73 pp.

Keshavamurty, R. N., 1982: Response of the atmosphere to sea surface temperature anomalies over the equatorial Pacific and the teleconnections of the Southern Oscillation. *J. Atmos. Sci.*, **39,** 1241–1259.

Lau, N. C., 1985: Modeling the seasonal dependence of the atmospheric response to observed El Niños in 1962–76. *Mon. Wea. Rev.*, **113,** 1970–1996.

Le Marshall, J. F., G. A. M. Kelly and D. J. Karoly, 1985: An atmospheric climatology of the Southern Hemisphere based on ten years of daily numerical analyses (1972–1982): I. Overview. *Aust. Meteor. Mag.*, **33,** 65–85.

Mo, K. C., and G. H. White, 1985: Teleconnections in the Southern Hemisphere. *Mon. Wea. Rev.*, **113,** 22–37.

——, and M. Ghil, 1987: Statistics and dynamics of persistent anomalies. *J. Atmos. Sci.*, **44,** 877–901.

Palmer, T. N., and D. A. Mansfield, 1986: A study of wintertime circulation anomalies during past El Nino events using a high resolution general circulation model. I: Influence of model climatology. *Quart. J. Roy. Meteor. Soc.*, **112,** 613–638.

Rasmusson, E. M., and T. H. Carpenter, 1982: Variations in tropical sea surface temperature and surface wind fields associated with

the Southern Oscillation/El Niño. *Mon. Wea. Rev.*, **110,** 354–384.

Swanson, G. S., and K. E. Trenberth, 1981: Trends in the Southern Hemisphere tropospheric circulation. *Mon. Wea. Rev.*, **109,** 1879–1889.

Szeredi, I., 1987: The structure of monthly fluctuations of the Southern Hemisphere troposphere. Ph.D. thesis, Monash University, 171 pp. [Available from Monash University, Clayton, Victoria 3168, Australia.]

——, and D. J. Karoly, 1987: The horizontal structure of monthly fluctuations of the Southern Hemisphere troposphere from station data. *Aust. Meteor. Mag.*, **35,** 119–129.

Trenberth, K. E., 1976: Spatial and temporal variations of the Southern Oscillation. *Quart. J. Roy. Meteor. Soc.*, **102,** 639–653.

van Loon, H., 1984: The Southern Oscillation. Part III: Associations with the trades and with the trough in the westerlies of the South Pacific Ocean. *Mon. Wea. Rev.*, **112,** 947–954.

——, and J. C. Rogers, 1981: The Southern Oscillation. Part II: Associations with changes in the middle troposphere in northern winter. *Mon. Wea. Rev.*, **109,** 1163–1168.

——, and D. J. Shea, 1987: The Southern Oscillation. Part IV: Anomalies of sea level pressure on the Southern Hemisphere and of Pacific sea surface temperature during the development of a warm event. *Mon. Wea. Rev.*, **115,** 370–379.

Wallace, J. M., and D. S. Gutzler, 1981: Teleconnections in the geopotential height field during the Northern Hemisphere winter. *Mon. Wea. Rev.*, **109,** 784–812.